Method for modeling decoherence on a quantum-information processor

G. Teklemariam,[1] E. M. Fortunato,[2] C. C. López,[3] J. Emerson[2] Juan Pablo Paz[3,*] T. F. Havel,[2] and D. G. Cory[2,†]
[1]*Department of Physics, Massachusetts Institute of Technology, Cambridge, Massachusetts 02139, USA*
[2]*Department of Nuclear Engineering, Massachusetts Institute of Technology, Cambridge, Massachusetts, 02139, USA*
[3]*Departamento de Física, "Juan Jose Giambiagi," Facultad de Ciencias Exactas y Naturales, Universidad de Buenos Aires, RA-1428 Buenos Aires, DF, Argentina*
(Received 15 January 2003; published 30 June 2003)

We develop and implement a method for modeling decoherence processes on an N-dimensional quantum system that requires only an N^2-dimensional quantum environment and random classical fields. This model offers the advantage that it may be implemented on small quantum-information processors in order to explore the intermediate regime between semiclassical and fully quantum models. We consider in particular $\sigma_z\sigma_z$ system-environment couplings which induce coherence (phase) damping, although the model is directly extendable to other coupling Hamiltonians. Effective, irreversible phase damping of the system is obtained by applying an additional stochastic Hamiltonian on the environment alone, periodically redressing it and thereby irreversibliy randomizing the system phase information that has leaked into the environment as a result of the coupling. This model is exactly solvable in the case of phase damping, and we use this solution to describe the model's behavior in some limiting cases. In the limit of small stochastic phase kicks the system's coherence decays exponentially at a rate that increases linearly with the kick frequency. In the case of strong kicks we observe an effective decoupling of the system from the environment. We present a detailed implementation of the method on a nuclear magnetic resonance quantum-information processor.

DOI: 10.1103/PhysRevA.67.062316 PACS number(s): 03.67.Lx, 03.65.−w, 03.65.Yz

I. INTRODUCTION

As early as the 1930s von Neumann [1] recognized that quantum correlations are crucial to understanding the quantum measurement process. He considered measurement as a process that first required correlating the system with the quantum apparatus through a unitary, information conserving, quantum evolution. To complete the measurement a mechanism was needed by which this pure, correlated state decayed into a mixture approximately diagonal in the basis of observation. In recent decades, the process of decoherence, which explains the dynamical origin of the above decay, has been extensively studied [2–5]. By employing an open-systems approach, the effect of the interaction between the measurement apparatus and its environment was included explicitly, and von Neumann's method was extended. The physical origin of the process of decoherence is very simple: the quantum correlations between the apparatus and the environment that are established in the course of their interaction is responsible for the dynamical selection of a preferred set of states of the apparatus (the pointer states). The mechanisms of decoherence are now a subject of great practical interest. Some of the recent work on decoherence includes the determination of emergent properties of pointer states [6,7], efforts to design specific pointer states by engineering the environment [8], and identification of the time scales of the decoherence process [9].

One of the simplest and most illustrative models of decoherence was originally suggested and studied by Zurek [5]. It consists of a two-level system (a spin 1/2 particle) coupled to n two-level systems through a $\sigma_z\sigma_z$ type interaction. With this model, in the large n limit, it is possible to show that the correlations which arise between the system and the environment lead to the damping of the system coherence, encoded in the off-diagonal elements of the density matrix. In this work we present results, both theoretical and experimental, for a two-level system that is coupled to a few other two-level systems, which shows that by manipulating the latter one can reproduce the essential features of Zurek's model.

Interest in this and other decoherence models (for example a two-level system coupled to a boson bath [10–12]) has grown over the last few years due to the development of quantum-information processing (QIP). A major challenge in QIP is the preservation of quantum coherence in the face of constant perturbations by an environment. While one could try to isolate the QIP device, this would make controlling the system difficult. Therefore, other strategies like quantum error correction [13] and noiseless subsystems [14–16] have been developed. The aim of this work is to develop methods to emulate decoherence in a physical setting, such as a QIP device, so that the nature and underlying physics of decoherence can be better understood and applied in the development of control strategies.

The paper is organized as follows. In Sec. II we introduce the essential features of decoherence, reviewing the model proposed by Zurek in which the system consists of a single spin while the environment is composed of an ensemble of n spins. In Sec. III we describe a simple model in which the environment is limited to only a few spins (qubits) and analyze a strategy through which these few spins can simulate a much larger effective environment. The strategy consists of randomly redressing the phase of the environment qubits

*Present address: Theoretical Division, MSB213, Los Alamos National Laboratory, Los Alamos, New Mexico 87545, USA.
†Author to whom correspondence should be addressed. Email address: dcory@mit.edu

during their interaction with the system and averaging over many realizations of this evolution. We describe an exact solution of this model in the case of a $\sigma_z\sigma_z$ coupling between the system and a single environment qubit. In this case we provide an analytic description of the decoherence (phase damping and decoupling) effects that arise under specific limiting conditions and also derive the associated Kraus operators for the model. A more detailed numerical analysis of this model is given for the case in which the environment consists of two qubits. In Sec. IV, we present nuclear magnetic resonance (NMR) QIP simulations for the two-qubit environment and comparisons of these results with the one- and two-qubit environment predictions and numerical simulations. In Sec. V, we summarize our results and discuss the extension of this model to more general decoherence mechanisms.

II. ZUREK'S DECOHERENCE MODEL

In this section we review the basic elements of quantum decoherence by presenting an open-system model due to Zurek [5] which is simple enough to be solved analytically. In spite of its simplicity the model captures many of the elements of decoherence theories and sheds insight into the loss of coherence, the onset of irreversibility, and in particular, the role played by the size of the environment.

Consider n two-level systems and focus on one system as the subsystem of interest. This subsystem interacts with the rest of the system through a bilinear interaction. The overall dynamics is described by

$$\mathcal{H}_{SE}=\sum_{k=2}^{n} J_{1k}\sigma_z^1\sigma_z^k, \tag{1}$$

where the system qubit is denoted by the superscript "1." This Hamiltonian is energy conserving and only causes phase damping. The prescription of the open-systems approach is to evolve the combined system and environment, represented by the density matrix $\rho^{SE}(t)$, and then recover the system density matrix from a partial trace over the environment degrees of freedom:

$$\rho^S(t)=\mathrm{Tr}_E\{\rho^{SE}(t)\}=\begin{pmatrix}\rho_{00}^S(t) & \rho_{01}^S(t)\\ \rho_{10}^S(t) & \rho_{11}^S(t)\end{pmatrix}. \tag{2}$$

In Eq. (2) $\rho_{00}^S(t)$ and $\rho_{11}^S(t)$ represent the system population terms while $\rho_{01}^S(t)=\rho_{10}^{S*}(t)$ represents the system coherence term. If the coherence terms vanish, the pure state is turned into a mixture in the computational basis (σ_z basis), i.e., a "pointer basis" has been selected out by *einselection*. An important observation is that, in the absence of a self-Hamiltonian, the system's statonary states are selected out by the interaction Hamiltonian. In fact, since $[\sigma_z,\mathcal{H}_{tot}]=0$, the interaction with the environment has two memory states $|0\rangle_S,|1\rangle_S$ as eigenstates and the populations remain unchanged throughout the system's evolution. The coupling in Eq. (1) is therefore a purely phase damping mechanism and there is no energy exchange between the system and environment.

The combined system evolves by the unitary propagator

$$\mathcal{U}_{SE}(t)=\exp(-i\mathcal{H}_{SE}t)=\exp\left(-i\sum_{k=2}^{n} J_{1k}\sigma_z^1\sigma_z^k t\right). \tag{3}$$

Consider a factorizable initial state of the combined system:

$$|\Phi(0)\rangle_{SE}=|\psi(0)\rangle_S\otimes|\psi(0)\rangle_E$$
$$=(a|0\rangle_1+b|1\rangle_1)\prod_{k=2}^{n}(\alpha_k|0\rangle_k+\beta_k|1\rangle_k). \tag{4}$$

The evolution is such that

$$|\Phi(t)\rangle_{SE}=a|0\rangle_1\prod_{k=2}^{n} e^{-iJ_{1k}\sigma_z^k t}|\phi\rangle_k+b|1\rangle_1\prod_{k=2}^{n} e^{iJ_{1k}\sigma_z^k t}|\phi\rangle_k, \tag{5}$$

where $|\phi\rangle_k=\alpha_k|0\rangle_k+\beta_k|1\rangle_k$. The interaction entangles the system states with the environment. In the language of QIP, the transformation $\mathcal{U}_{SE}$ generates a conditional phase gate between the system and its environment, conditioned on the system's state. After the interaction the state is

$$|\Phi(t)\rangle_{SE}=a|0\rangle_1\prod_{k=2}^{n}[\alpha_k e^{-iJ_{1k}t}|0\rangle_k+\beta_k e^{iJ_{1k}t}|1\rangle_k]$$
$$+b|1\rangle_1\prod_{k=2}^{n}[\alpha_k e^{iJ_{1k}t}|0\rangle_k+\beta_k e^{-iJ_{1k}t}|1\rangle_k] \tag{6}$$

and reflects the fact that the system and environment states are not factorizable. The off-diagonal element of the system's reduced density matrix (system coherence) is

$$\rho_{01}^S(t)={}_1\langle 0|\mathrm{Tr}_E\{|\Phi(t)\rangle_{SE}\langle\Phi(t)|_{SE}\}|1\rangle_1, \tag{7}$$

so that

$$\rho_{01}^S(t)=ab^*z(t), \tag{8}$$

where

$$z(t)=\prod_{k=2}^{n}[|\alpha_k|^2e^{-2iJ_{1k}t}+|\beta_k|^2e^{2iJ_{1k}t}]. \tag{9}$$

Recall that a and b are the coefficients of the initial pure state of the system.

The time dependence of $z(t)$ contains the crucial information for understanding the behavior of the system coherence. In particular, the magnitude of $z(t)$ determines the damping of the phase information originally contained in $\rho_{01}(0)$, with $|z(t)|\to 0$ reflecting nonunitary evolution and "irreversibility."

For a finite system, $|z(t)|$ is at worst quasiperiodic and one can always define a recurrence time τ_E. The existence of such a recurrence time reflects the fact that the information loss is in principle recoverable. In the continuum limit, $n\to\infty$, $z(t)$ is no longer quasiperiodic and $\tau_E\to\infty$. The phase

information is then unrecoverably lost, displaced from the degrees of freedom of the system to the infinitely many degrees of freedom of the environment.

To characterize the degree of decoherence one can consider the size of the fluctuations of $z(t)$ around its time-averaged mean value $\langle z(t)\rangle = 0$:

$$\langle |z(t)|^2 \rangle = \lim_{T\to\infty} \frac{1}{T} \int_0^T dt' |z(t')|^2$$

$$\approx \frac{1}{2^{n-1}} \prod_{k=2}^{n} [1 + (|\alpha_k|^2 - |\beta_k|^2)^2]. \qquad (10)$$

Thus, typical fluctuations vary as $1/\sqrt{\dim \mathcal{H}_E}$, and the effectiveness of the decoherence mechanism in this model is determined by the dimension of the environment.

To summarize, the key features of this model of decoherence are as follows. (1) The system of interest evolves through a direct entangling interaction with each two-level system in a very large environment, and at any time the (reduced) density matrix of the system is obtained from a trace over the environment degrees of freedom. (2) Expressed in the pointer basis of the system, which in this simplest case is the set of states that commute with the interaction Hamiltonian, the reduced density matrix becomes approximately diagonal and the off-diagonal elements exhibit coherence loss. (3) The fluctuations of the decoherence produced by this model, measured by the size of the system's off-diagonal elements, are controlled by the dimension of the environment's Hilbert space.

III. A HIERARCHICAL DECOHERENCE MODEL

We consider the problem of experimentally simulating quantum decoherence in a physical setting in which limited quantum resources are available for modeling the quantum environment. By ''simulating quantum decoherence'' we are referring not only to the challenge of implementing an arbitrary open-system trajectory on a QIP device, but also to the study of the decoherence processes that result from specific system-environment couplings (for example, derived from a model of some physical system of interest).

As in Zurek's model the exclusive direct mechanism for system decoherence in our model is the coupling between the system and a local quantum environment through a fixed bilinear Hamiltonian. However, our model of decoherence has two features distinct from the model described above. The first difference is a constraint on the Hilbert space size derived from practical considerations: we allow the dimension of the Hilbert space for the local quantum environment to be no larger than N^2, where N is the dimension of the Hilbert space of the system. In this way the quantum environment is the smallest size that will enable the implementation of an arbitary completely positive map on the system through a unitary operator on the combined system and environment. To remove the information from our finite quantum environment we include a stochastic classical field in our model. This strategy is designed to eliminate the quantum back action from low dimensional environments. Basically, the technique consists of redressing [17] the environment's quantum state by applying a sequence of random classical kicks to the environment qubits, and then averaging over realizations of this stochastic noise. This has the effect of scrambling the system information after it has been stored in the quantum environment through the coupling interaction. It is worth stressing that the system itself is not subjected to these classical kicks and the associated stochastic averaging. This model, and the associated method realized in this paper, is depicted schematically in Fig. 1. A generalization of this method to provide a time-dependent open-system

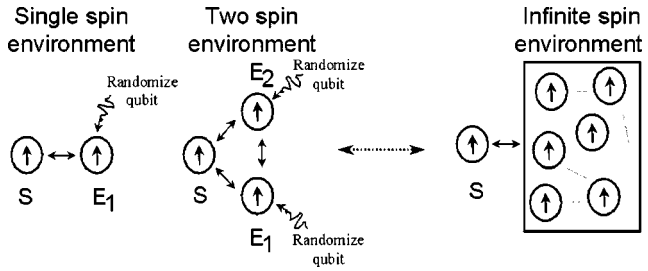

FIG. 1. The schematics on the left describe the models developed in this paper. A single spin system S is coupled to one- and two-spin quantum environments, designated E_i. During the coupling the system phase information leaks into the environment. Since the spin environment is finite, in order to simulate the effects of a larger quantum environment (depicted on the right), a mechanism is needed by which the information stored in the available quantum environment can be effectively erased. We accomplish this by redressing the environment degrees of freedom with stochastic phase kicks.

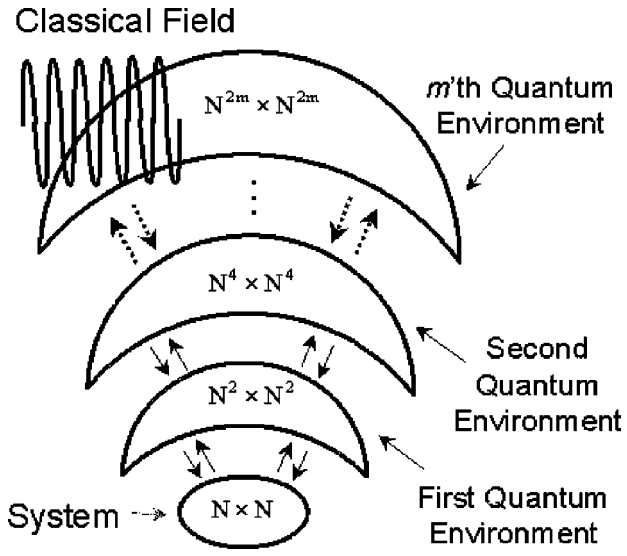

FIG. 2. A schematic of the system coupled to a hierarchy of quantum environments, as resources permit, and the role of the classical stochastic field. Each environment is coupled only locally (to its neighbors in the hierarchy). It should be noted that the classical environment interacts only with the quantum environments, and does not interact directly with the quantum system. In this paper we consider only the case of one local quantum environment, as portrayed in Fig. 1.

evolution is described in the discussion and depicted in Fig. 2.

As we shall show below, this scheme enables simulation of the quantum decoherence that normally arises for much larger effective environment sizes. In particular, we demonstrate the simulation of phase damping on a NMR QIP consisting of three qubits (see Fig. 1). In the NMR simulation, the system is represented by one qubit while the other two qubits represent the quantum environment. Before turning to a discussion of the three-qubit experiment, we first describe and analyze this simulation method theoretically in the simplest and solvable case of the phase damping of a single system qubit from a single environment qubit (also depicted in Fig. 1).

A. One-qubit environment: Simple solvable model

Below we introduce the essential features of this decoherence model by considering an exact solution available in the case of a one-qubit environment coupled to the system by a $\sigma_z\sigma_z$ interaction. With the system and environment qubits labeled by S and E, respectively, the full Hamiltonian is given by

$$\mathcal{H}_0=\pi\left(\nu_S\sigma_z^S+\nu_E\sigma_z^E+\frac{\Omega}{2}\sigma_z^S\sigma_z^E\right). \tag{11}$$

Here, ν_S, ν_E, and Ω are frequencies in units of hertz. This Hamiltonian includes both the self-evolution of the two qubits and their interaction. In the absence of any other interaction, the evolution operator for a time t is

$$U(t)=\exp\left[-i\pi\left(\nu_S\sigma_z^S+\nu_E\sigma_z^E+\frac{\Omega}{2}\sigma_z^S\sigma_z^E\right)t\right]. \tag{12}$$

We will consider the evolution of this system subject to a sequence of kicks that affect only the environment qubit. Every kick is generated by a transverse magnetic field that rotates the environment qubit around the y axis by an angle ϵ_m chosen randomly in the interval $(-\alpha,+\alpha)$. The evolution operator for the mth kick is given by $K_m=I^S\otimes K_m^E$, where

$$K_m^E=\exp(-i\epsilon_m\sigma_y^E) \tag{13}$$

and I is the identity matrix. In our proposed model, the kicks are considered instantaneous; therefore, the evolution for a total time $T=n/\Gamma$, where Γ is the kick rate, can be written

$$U_n(T)=K_nU\left(\frac{T}{n}\right)K_{n-1}U\left(\frac{T}{n}\right)\cdots K_1U\left(\frac{T}{n}\right). \tag{14}$$

It is useful to keep in mind that the operator $U_n(T)$ depends also on the values of the random variables ϵ_m $(m=1,\ldots,n)$ corresponding to the kick angles.

Our goal is to obtain a closed expression for the reduced density matrix of the system qubit for an ensemble of realizations of the random variables ϵ_m. The density matrix for this ensemble is given by

$$\overline{\rho^S(T)}=\int_{-\alpha}^{\alpha}\frac{d\epsilon_n}{2\alpha}\cdots\int_{-\alpha}^{\alpha}\frac{d\epsilon_1}{2\alpha}\mathrm{Tr}_E[U_n\rho^{SE}(0)U_n^\dagger], \tag{15}$$

where α is the spread of allowed kick angles over which the $\epsilon_m(m=1,\ldots,n)$ are uniformly distributed. We will consider a factorizable initial state for the two qubits (this is not essential):

$$\rho^{SE}(0)=\rho^S(0)\otimes\rho^E(0). \tag{16}$$

It is convenient to express the initial density matrix of the system in the basis of eigenstates of σ_z,

$$\rho^S(0)=\sum_{j,l=0,1}\rho_{jl}^S(0)|j\rangle\langle l|. \tag{17}$$

Then we can simplify the expression for $U_n(T)$. To do this, we evaluate the effect of the first step in the evolution Eq. (14) as follows:

$$\begin{aligned}\rho^{SE}(1)&=K_1U(T/n)\rho^{SE}(0)U(T/n)^\dagger K_1^\dagger\\&=\sum_{j,l=0,1}[\rho_{jl}^S(0)|j\rangle\langle l|]\otimes[K_1^EV_j^E\rho^E(0)(K_1^EV_l^E)^\dagger],\end{aligned} \tag{18}$$

where we have defined the environment operator

$$\begin{aligned}V_j^E&=\left\langle j\left|U\left(\frac{T}{n}\right)\right|j\right\rangle\\&=\exp\left[-i\frac{\pi}{\Gamma}\nu_S(-1)^j-i\frac{\pi}{\Gamma}\left(\frac{\Omega}{2}(-1)^j+\nu_E\right)\sigma_z^E\right].\end{aligned} \tag{19}$$

In the above we have explicitly evaluated the action of the interaction Hamiltonian on the system states, and the j dependence of the single step operator V_j^E reflects the fact that it operates on the environment state conditionally on the system state. The important point is that the evolution operators for the additional $n-1$ iterations will factor as above, producing a final expression with (conditional) operators that act exclusively on the environment qubit. Hence, we can immediately obtain the following simple form for the final density matrix of the system qubit:

$$\overline{\rho^S(T)}=\sum_{j,l=0,1}\rho_{jl}(0)f_{jl}(n,T)|j\rangle\langle l|, \tag{20}$$

where the function $f_{jl}(n,T)$, which we call the *decoherence factor*, carries all the information about the effect of the environment qubit on the system qubit, including also the trivial phases from the system's self-evolution. It is given by the formula

$$f_{jl}(n,T)=\int_{-\alpha}^{\alpha}\frac{d\epsilon_n}{2\alpha}\cdots\int_{-\alpha}^{\alpha}\frac{d\epsilon_1}{2\alpha}\mathrm{Tr}_E[(A_j^E)_n\rho^E(0)(A_l^E)_n^\dagger], \tag{21}$$

where the operator $(A_j^E)_n n$ is defined as

$$(A_j^E)_n = \langle j|U_n(T)|j\rangle = K_n^E V_j^E K_{n-1}^E V_j^E \cdots K_1 V_j^E . \quad (22)$$

It is clear from Eq. (21) that for $j=l$ the final trace over the environment system is equal to 1 and therefore we always have $f_{jj}=1$. Thus, this decoherence model affects only the off-diagonal terms in the σ_z basis, in other words, the σ_z eigenbasis is a pointer basis.

The remaining task is to evaluate the decoherence factor $f_{01}(n,T)$ since on general grounds one can show that $f_{jl}(n,T)=f_{lj}(n,T)^*$. To evaluate $f_{jl}(n,T)$ it is convenient to notice that the integrals in Eq. (21) can be brought forward through the independent operator terms in the sequence in Eq. (22), and the evolution can be expressed as the successive application of a superoperator on the initial density matrix of the environment $\rho^E(0)$. Thus, we can write

$$f_{01}(n,T) = \mathrm{Tr}_E[\mathcal{O}^n(\rho^E(0))], \quad (23)$$

where the superoperator $\mathcal{O}$ is defined as

$$\begin{aligned}\mathcal{O}(\rho) &= \int_{-\alpha}^{\alpha} \frac{d\epsilon}{2\alpha} K^E V_0^E \rho (V_1^E)^\dagger (K^E)^\dagger \\ &= e^{-2i\pi\nu_S T/n} \int_{-\alpha}^{\alpha} \frac{d\epsilon}{2\alpha} e^{-i\epsilon\sigma_y} e^{-i\pi(\Omega/2+\nu_E)T\sigma_z/n} \\ &\quad \times \rho e^{-i\pi(\Omega/2-\nu_E)T\sigma_z/n} e^{i\epsilon\sigma_y}. \end{aligned} \quad (24)$$

The dependence of f_{01} on the self-evolution of the system factors out as a phase factor that modulates the overall evolution in Eq. (24). This trivial phase factor will be omitted from here on because it can be easily restored if necessary. After integrating over the random variable the last expression becomes

$$\begin{aligned}\mathcal{O}(\rho) &= c(e^{-i\pi(\Omega/2+\nu_E)T\sigma_z/n} \rho e^{-i\pi(\Omega/2-\nu_E)T\sigma_z/n}) \\ &\quad + d(\sigma_y e^{-i\pi(\Omega/2+\nu_E)T\sigma_z/n} \rho e^{-i\pi(\Omega/2-\nu_E)T\sigma_z/n} \sigma_y), \end{aligned} \quad (25)$$

where $\gamma = c-d = \sin(2\alpha)/2\alpha$ and $c+d=1$. It is worth stressing that this superoperator is not trace preserving or Hermitian. It is easy to show that $\mathcal{O}(\sigma_x)$ and $\mathcal{O}(\sigma_y)$ are linear combinations of σ_x and σ_y. Similarly, $\mathcal{O}(I)$ and $\mathcal{O}(\sigma_z)$ are written as linear combinations of I and σ_z. The decoherence factor f_{01} is given following a final trace over the environment qubit. So the traceless terms in $\rho^E(0)$, those proportional to σ_x and σ_y, do not contribute to the final result. Therefore, to compute $f_{01}(n,T)$ the superoperator $\mathcal{O}$ is applied n times to the part of the initial state with components along the identity and σ_z. Writing the initial density matrix of the environment qubit as $\rho^E(0)=(I+p_x\sigma_x+p_y\sigma_y+p_z\sigma_z)/2$, we obtain

$$f_{01}(n,T) = \frac{1}{2}\mathrm{Tr}[O^n(I)] + \frac{1}{2} p_z \,\mathrm{Tr}[O^n(\sigma_z)]. \quad (26)$$

The actions of $\mathcal{O}$ on the identity and σ_z are

$$\mathcal{O}(I) = \cos(\pi\Omega T/n) I - i\gamma \sin(\pi\Omega T/n)\sigma_z ,$$

$$O(\sigma_z) = -i \sin(\pi\Omega T/n) I + \gamma \cos(\pi\Omega T/n)\sigma_z .$$

Note that the above expressions have no dependence on the frequencies ν_S and ν_E since they came in as trivial phase factors.

The eigenvalues λ_1 and λ_2 (and the corresponding eigenvectors) of the superoperator $\mathcal{O}$ can be obtained directly, giving

$$\lambda_2^1 = \frac{1}{2}(1+\gamma)\cos(\pi\Omega T/n) \pm \sqrt{\frac{(1+\gamma)^2}{4}\cos^2(\pi\Omega T/n) - \gamma}, \quad (27)$$

and, from them one can find the following exact solution:

$$\begin{aligned} f_{01}(n,T) &= \frac{\cos(\pi\Omega T/n)(\lambda_1^n - \lambda_2^n) + \lambda_1\lambda_2^n - \lambda_2\lambda_1^n}{(\lambda_1-\lambda_2)} \\ &\quad - i p_z \sin(\pi\Omega T/n) \frac{(\lambda_1^n - \lambda_2^n)}{(\lambda_1-\lambda_2)}. \end{aligned} \quad (28)$$

Notice that this formula is an explicit expression (obtained with no approximations) valid for all values of the parameters defining our model (n, γ, etc). Also, it is worth stressing that the dependence on the initial state of the environment (entering the above equation through the initial polarization p_z) is rather trivial. Moreover, the first and second lines of the last equation clearly separate the real and imaginary parts of the decoherence factor f_{01}. Below, we will analyze the predictions of this model for some simple cases.

1. Dependence on kick angle: Limiting cases

We first consider the dependence of the decoherence factor f_{01} on γ. Let us consider three cases. First we discuss the limit $\gamma=1$, which corresponds to unitary evolution (that is, no kicks since the kick angle $\alpha=0$). Then, we consider the case $\gamma=0$, which corresponds to averaging over angles between 0 and 2π. Finally, we analyze in some detail the case where γ is close to 1 (small angle kicks), which is the condition met in our simulations and experiments. In all these cases the decoherence factor f_{01} is directly related to observable quantities $\langle\sigma_x^S\rangle = 2\,\mathrm{Re}[\rho_{01} f_{01}]$ and $\langle\sigma_y^S\rangle = 2\,\mathrm{Im}[\rho_{01} f_{01}]$.

Unitary evolution: $\gamma=1$. This is the simplest case. Here, the superoperator $\mathcal{O}$ is such that $\mathcal{O}(\rho)=\rho\exp(-i\pi\Omega T\sigma_z/n)$ for any operator ρ that is a linear combination of the identity and σ_z. Recall that we showed earlier that σ_x and σ_y are eigenvectors of $\mathcal{O}$ and thus vanish after the trace. Using this, or simply replacing $\gamma=1$ in the decoherence factor [Eq. (28)],

$$f_{01}(n=0,T) = \cos(\pi\Omega T) - i p_z \sin(\pi\Omega T). \quad (29)$$

This has a clear physical interpretation. The decoherence factor is independent of the kicking rate (as it should be since there are no kicks in this limit). Recall that p_z is the initial

polarization of the environment qubit; therefore the system qubit rotates independently of the environment qubit.

Complete randomization: $\gamma=0$. Here the kick angles ϵ_j vary over the entire interval between 0 and 2π. In this case the above formulas simplify substantially to

$$f_{01}(\Gamma,T)=\cos^{\Gamma T}\left(\frac{\pi\Omega}{\Gamma}\right)-ip_z\sin\left(\frac{\pi\Omega}{\Gamma}\right)\cos^{\Gamma T-1}\left(\frac{\pi\Omega}{\Gamma}\right), \tag{30}$$

where use of $n=\Gamma T$ was made. (Recall that $\Gamma=n/T$ is the kick rate.) In the large Γ limit we clearly see a Zeno-like effect (for an operator, not a state) which can be obtained from Eq. (30) by noting that

$$\cos^{\Gamma T}\left(\frac{\pi\Omega}{\Gamma}\right)\approx\left[1-\frac{1}{2}\left(\frac{\pi\Omega}{\Gamma}\right)^2\right]^{\Gamma T}\approx\exp\left(-\frac{(\pi\Omega)^2T}{2\Gamma}\right). \tag{31}$$

Thus, in this limit for faster kick rates Γ the system takes longer to decohere.

Average over small angles: $\gamma=1-O(\alpha^2)$. Here we consider the case where the averaging is over small angles (the regime we consider in the simulations and experiments is $\alpha=\pi/20$), where

$$\gamma\approx1-\frac{2}{3}\alpha^2. \tag{32}$$

Defining $\epsilon=\frac{2}{3}\alpha^2$, we can expand both eigenvalues in powers of ϵ to obtain an expression which is valid for small $n=\Gamma T$:

$$f_{01}(\Gamma,T)=\left(1-\frac{\epsilon}{2}\right)^{\Gamma T}\left(1+\frac{\epsilon}{2}\right)[\cos(\pi\Omega T)-ip_z\sin(\pi\Omega T)+O(\epsilon)]. \tag{33}$$

In this regime the envelope of the decay of f_{01} is exponential with a decay rate proportional to the kick rate because $\epsilon\ll1$ implies $(1-\epsilon/2)^n\approx\exp(-n\epsilon)$. The analysis of the exact formula shows that in this case (large n) a Zeno-type effect arises (as before).

The dependence of the decay rate T_2 the kicking rate is shown in Fig. 3. The numerical data in the figures are obtained from the exact expression for f_{01}. The initial state for the system qubit is taken to be $\rho^S=\frac{1}{2}(I+\sigma_x)$, in which case f_{01} is directly proportional to the transverse polarization of the qubit. For small values of the kick rate $1/T_2$ is linear in Γ. However for larger values $1/T_2$ saturates and decays again due to the Zeno-like effect. These results substantiate our expectation that the kick rate can be applied to control the attenuation of the recurrences. In the low kick rate limit the role of the kick rate is analogous to the variable environment size in Zurek's model.

2. Kraus forms

For a one-spin environment a phase damping channel can be represented by a purification basis [18,19] that evolves the system and environment with the unitary operator:

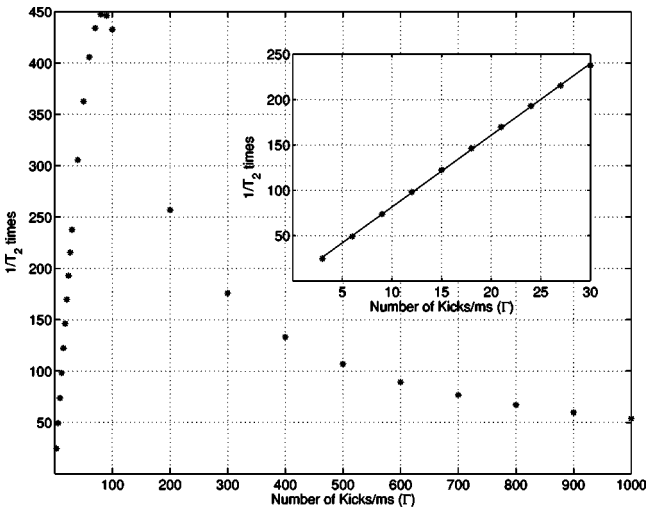

FIG. 3. The decay rate as a function of the kick rate Γ. For $\Omega=300$ Hz and $\gamma=0.98$, the kicking is no longer effective at inducing decoherence beyond a kick rate of about 50 kicks/ms. Only kick rates up to 1000 kicks/ms are shown, and after 5000 kicks/ms the decay is no longer exponential. Inset: the decay rate as a function of the kick rate is linear for small values of Γ. The plot is for $\Omega=300$ Hz and $\gamma=0.98$.

$$\mathcal{U}_{SE}=e^{-i\theta\sigma_z^S\sigma_y^E}=E_+^Se^{-i\theta\sigma_y^E/2}+E_-^Se^{i\theta\sigma_y^E/2}, \tag{34}$$

where $E_\pm^S=\frac{1}{2}(I\pm\sigma_z^S)$, or equivalently $E_+=|0\rangle\langle0|$ and $E_-=|1\rangle\langle1|$. This operator transforms the states of $\rho^{SE}(0)=\rho^S(0)\otimes E_+^E$ as follows:

$$|0\rangle_S|0\rangle_E\xrightarrow{\mathcal{U}}\cos(\theta/2)|0\rangle_S|0\rangle_E+\sin(\theta/2)|0\rangle_S|1\rangle_E,$$

$$|1\rangle_S|0\rangle_E\xrightarrow{\mathcal{U}}\cos(\theta/2)|1\rangle_S|0\rangle_E-\sin(\theta/2)|1\rangle_S|1\rangle_E. \tag{35}$$

By tracing away the environment states ($\mathcal{H}_E:\{|0\rangle_E,|1\rangle_E\}$) this channel has the Kraus operator sum representation [20–22] given by

$$\hat{\mathcal{S}}(\rho^S)=\hat{M}_0\rho^S\hat{M}_0+\hat{M}_1\rho^S\hat{M}_1, \tag{36}$$

where

$$\hat{M}_0=\cos(\theta/2)I^S,\quad \hat{M}_1=\sin(\theta/2)\sigma_z^S, \tag{37}$$

and $\hat{\mathcal{S}}$ is the superoperator map,

$$\hat{\mathcal{S}}(\rho^S)=\begin{bmatrix}\rho_{00}^S & \beta\rho_{01}^S\\ \beta\rho_{10}^S & \rho_{11}^S\end{bmatrix}, \tag{38}$$

with $\beta=\cos^2(\theta/2)-\sin^2(\theta/2)$. If we parametrize

$$\cos(\theta/2)\equiv\sqrt{\frac{1}{2}(1+f_{01})},\quad \sin(\theta/2)\equiv\sqrt{\frac{1}{2}(1-f_{01})}, \tag{39}$$

then we obtain the Kraus operator sum representation for the phase damping channel in our model:

$$\hat{\mathcal{S}}(\rho^S)=\frac{1}{2}(1+f_{01})\rho^S+\frac{1}{2}(1-f_{01})\sigma_z^S\rho^S\sigma_z^S. \quad (40)$$

From the analytical solution to the two-qubit model we see that a single qubit environment interacting with a single qubit system is sufficient to represent the phase-damping channel. Similarly, an N-dimensional system interacting with an environment of dimension N through the $\sigma_z\sigma_z$ interaction is sufficient to describe the open-system dynamics of phase damping. This is because dephasing is a special case where the Lie algebra of the noise consists of only the two operators σ_z and I (out of a possible four). In contrast, for an arbitrary completely positive map the dimension of the environment must be at least N^2 for a system with dimension N to induce an arbitrary mapping on the system.

B. Two-qubit environment: Numerical simulation

In the more general case where we wish to implement any completely positive map [20,21] on a one-qubit system the minimum required environment is two qubits. We therefore want to consider a two-qubit environment model. Moreover, we want to examine the effect of only a finite number of realization of the random kick variables. Therefore, a three-qubit model is explored numerically below. The results of a NMR QIP simulation [23,24] of this model are presented in the next section.

We now consider the following system-environment Hamiltonian:

$$\mathcal{H}_{tot}=\mathcal{H}_S+\mathcal{H}_E+\mathcal{H}_{SE}+\mathcal{H}_{E_1E_2}, \quad (41)$$

where

$$\mathcal{H}_S=\pi\nu_S\sigma_z^S,$$

$$\mathcal{H}_E=\pi\sum_{i=1}^{2}\nu_{E_i}\sigma_z^{E_i},$$

$$\mathcal{H}_{SE}=\frac{\pi}{2}\sum_{i=1}^{2}J_{SEi}\sigma_z^S\sigma_z^{Ei},$$

$$\mathcal{H}_{E_1E_2}=\frac{\pi}{2}J_{E_1E_2}\sum_{i=x,y,z}\sigma_i^{E_1}\sigma_i^{E_2}.$$

The environment spins E_1 and E_2 are also subjected to periodic, instantaneous kicks with an evolution operator of the form

$$\mathcal{K}_m=\exp\left[\sum_{i=1}^{2}\theta_i^m\sigma_y^{Ei}\right], \quad (42)$$

where the θ_i^m are the random values of the mth kick. The instantaneous nature of the kicks allows the evolution of the full system over the time interval T, with n instantaneous kicks, to be described by the operator

TABLE I. Parameters for the model Hamiltonian of Eq. (41).

$\nu_S=0$
$\nu_{E_1}=630$ Hz
$\nu_{E_2}=-630$ Hz
$J_{SE_1}=250$ Hz
$J_{SE_2}=50$ Hz
$J_{E_1E_2}=174$ Hz
$\theta=\{-\pi/20,+\pi/20\}$ (randomly chosen)

$$\mathcal{U}_n=\mathcal{K}_n\exp[-i\mathcal{H}_{tot}(T/n)]\mathcal{K}_{n-1}\exp[-i\mathcal{H}_{tot}(T/n)]\times\cdots\times\mathcal{K}_1\exp[-i\mathcal{H}_{tot}(T/n)], \quad (43)$$

where each $\mathcal{K}_m$ has a different random kick variable.

The resultant system density matrix for a single realization is now obtained by tracing out the environment. As before, we are interested in the system coherence as expressed through the off-diagonal elements of the system state in the basis of the pointer states,

$$\langle 0|\rho^S(T)|1\rangle=\langle 0|\,\mathrm{Tr}_{E_1E_2}[\mathcal{U}_n\rho^{SE_1E_2}(0)\mathcal{U}_n^\dagger]|1\rangle. \quad (44)$$

Finally, we must average over different realizations of the random variables, which gives the quantity $\{\langle 0|\rho^S|1\rangle\}$, where the curly brackets on $\langle 0|\rho^S|1\rangle$ denote the average over the finite number of realizations.

In order to simulate the physical system used in the NMR study, we have selected the parameter values presented in Table I. The system and environment were initialized in the state $\sigma_x^S E_+^{E_1}E_+^{E_2}$ and we simulated the evolution of the system on MATLAB. We ran ten different kick rates that ranged from 3 kicks/ms to 30 kicks/ms in steps of 3. The kicks were sampled from a uniform distribution of angles that ranged between $-\pi/20$ and $\pi/20$. The series was run for 150 ms. We averaged over 50 realizations and obtain the plots shown in Fig. 4. As shown in Fig. 5, the late-time oscillations reflect the finite number of realizations of the random variables. The envelope of the decays in Fig. 4 was fitted to an exponential, and the decay constants exhibited a linear dependence on the kick rate for small kick rates, as expected from the analytic solution (see Fig. 6). At about 900 kicks/ms the decay rates start decreasing with increasing kick rate and the system starts to become decoupled from the environment, an effect noted earlier in Eq. (30). This is the well-known decoupling phenomenon in NMR [25]. The onset of decoupling occurs when the rms angle of the stochastic kicks approaches a rotation of π (critical damping). The rms angle is given by the typical kick size $\simeq\pi/10$ times the square root of the number of kicks over a cycle time $\simeq 1/2J$ of the system-environment interaction. For the strongest system-environment coupling, $J\simeq 250$ Hz, the onset of decoupling is expected at a kick rate of 800 kHz, in good agreement with the numerical results (see Fig. 6).

IV. THE NMR IMPLEMENTATION

In this section, we describe the experimental implementation of our model. We chose propyne as the physical system

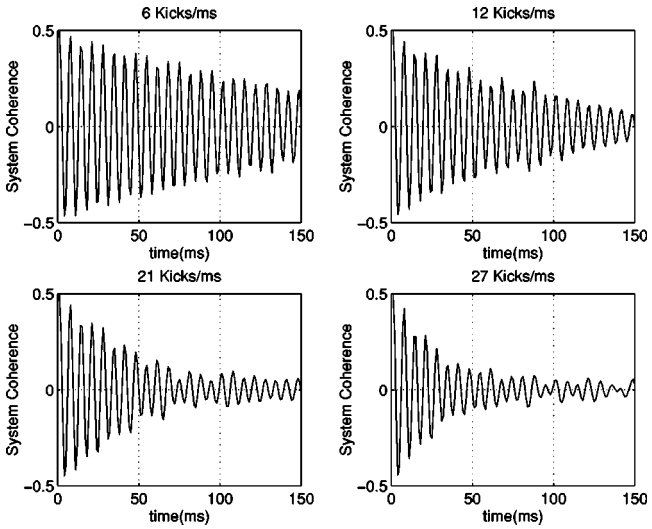

FIG. 4. Some example decays of the system coherence given by $\{\langle 0|\rho^S|1\rangle\}$ obtained from numerical simulation using MATLAB for 50 realizations of the random kick variables. The kick rates for each subplot are labeled above the figures. In this range the envelope of the decay is exponential (see inset to Fig. 6 below). We note that a higher kick rate leads to a faster system decay.

(see Fig. 7 for the internal Hamiltonian parameters). The hydrogen indicated with a circled 1 represents the system qubit and the two carbons labeled with a circled 2 and a circled 3 represent the environment qubits E_1 and E_2, respectively. These spin-1/2 nuclei have a large resonance frequency offset, so the hydrogen and carbon can be addressed and detected separately. The relatively large couplings present among these nuclei imply that the interactions take place over short times, and the long relaxation times allow one to observe the hydrogen signals over a relatively long time span without significant natural decay. The experiments were carried out on a liquid solution of propyne using a

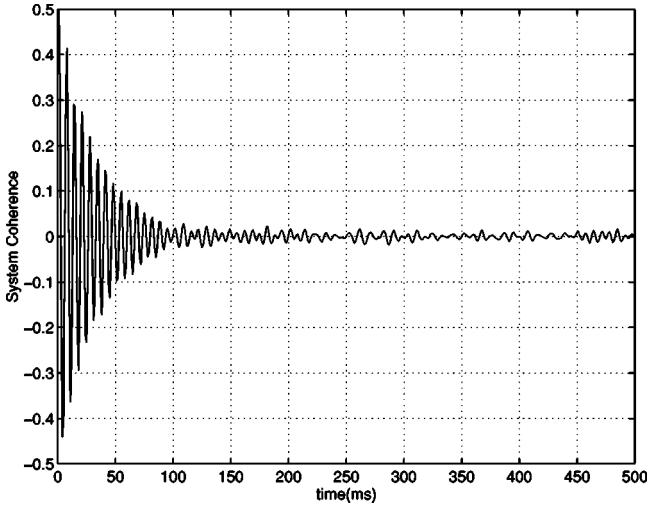

FIG. 5. A numerical simulation to demonstrate the suppression of revivals at longer times and higher averages. The times go out to 500 ms and the averages are taken for 200 realizations. Note that the revivals that seem prevalent in Figs. 4 and 8 are diminished.

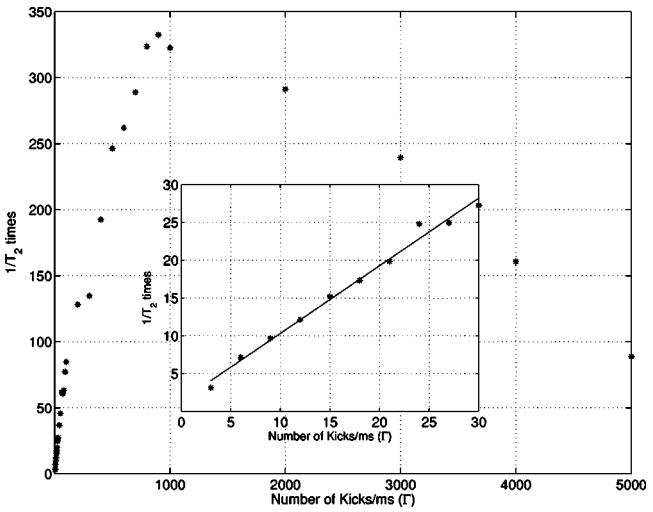

FIG. 6. Numerical simulation of the decoherence rate and the decoupling limit. Beyond a kick frequency of about 900 kicks/ms the decoherence rate from the kicking starts to decrease. This transition to a decoupling effect is described in the text. After about 5000 kicks/ms the decays are no longer exponential. Inset: demonstration of the proportionality between decoherence rate and kick rate for low kick rates. This linear relationship can be understood from the analytic results obtained for the one-qubit environment.

Bruker Avance spectrometer. Neglecting the methyl group (because it couples in very weakly), the internal Hamiltonian for propyne is given to a good approximation by

$$\mathcal{H}_{int} = \pi[\,\nu_1\sigma_z^1 + \nu_2\sigma_z^2 + \nu_3\sigma_z^3 + \tfrac{1}{2}\,(J_{12}\sigma_z^1\sigma_z^2 + J_{23}\sigma^2\cdot\sigma^3 + J_{13}\sigma_z^1\sigma_z^3)], \quad (45)$$

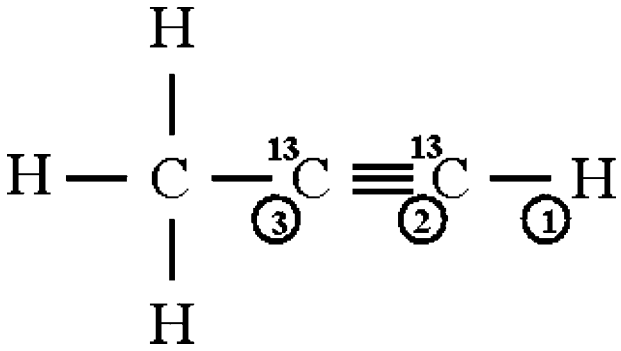

FIG. 7. The propyne molecule. The circled labels on the ^{13}C atoms and the rightmost hydrogen index the spins used in the experiment. The methyl group consists of three hydrogen atoms and an unlabeled carbon. In the experiments the field of the spectrometer was $\sim$9.2 T and the hydrogen resonances were $\sim$400 MHz while the carbon resonances were around $\sim$100 MHz. The chemical shift difference between the two labeled carbons is 1.260 kHz. Using the indexing scheme in the figure the J coupling constants are as follows: $J_{12}=246.5$ Hz, $J_{23}=173.8$ Hz, and $J_{13}=51.8$ Hz. The longitudinal relaxation times are $T_1^1=8.7$ s, $T_1^2=23$ s, and $T_1^3=43$ s, while the transverse relaxation times are $T_2^1=1.1$ s, $T_2^2=1.9$ s, and $T_2^3=1.7$ s.

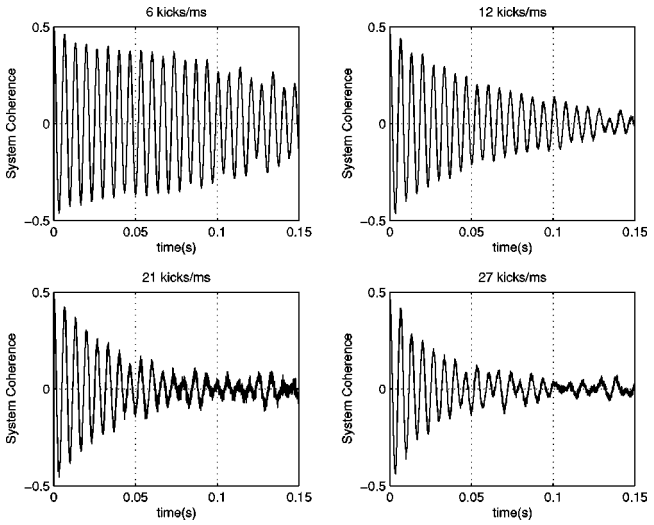

FIG. 8. Example decays from the experiment. The hydrogen signal was directly detected and the real part of the complex signal was plotted. The fluctuations at the tail end of the higher kick rates are due to low statistics. This was confirmed by comparing with simulations at higher averages. (See Fig. 5.)

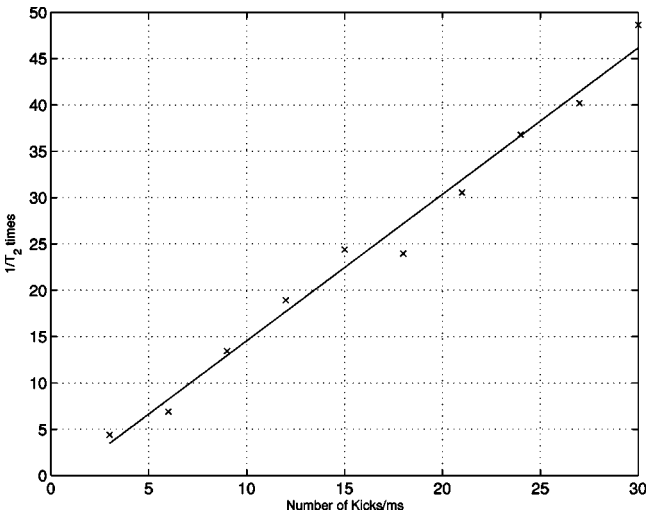

FIG. 9. The linear dependence of the experimental decay constants on kick rate. The data point symbols ($\times$) are larger than the error bars, which range from ± 0.0075 to ± 0.0573. Compared to the slope in the simulations of Fig. 6, the experimental slope reflects faster decay. This disparity is due to the slight differences between the experiment and simulations.

where the ν's are the Larmor frequencies and the J's the spin-spin coupling constants in hertz (the various values are given in Fig. 7). Equation (45) should be compared with Eq. (41). The nonsecular coupling between the carbon nuclei can be observed in the carbon spectra but has a negligible effect on the relevant experimental results.

A convenient choice for the initial state of system and environment is one where hydrogen is in a superposition state and both carbons are in an eigenstate. By placing the methyl hydrogens in an eigenstate as well, they can be eliminated from playing a role in the hydrogen spin dynamics. This was accomplished by using a highly selective rf pulse that irradiated a spectral line corresponding to the state

$$\sigma_x^{\mathrm{H}} E_+^{\mathrm{C1}} E_+^{\mathrm{C2}} E_+^{M}, \tag{46}$$

where $E_+ = \frac{1}{2}(I+\sigma_z)$, H represents hydrogen, C1 carbon 1, C2 carbon 2, and M the methyl hydrogen atoms. For this implementation we used a 5.5 s EBURP1 [26,27] pulse. The spectral resolution of this pulse was 0.5 Hz, and its design is such that it only generates a uniform excitation profile in the specified bandwidth. Ultimately, only $\sim 1/10$ of the maximum intensity was excited. Nonetheless, this yielded sufficient signal-to-noise ratio to carry out the experiments.

The observed hydrogen signal corresponds to $\langle \sigma_x^H(t) + i\sigma_y^H(t) \rangle$ and is equivalent to tracing away the carbons. The peaks of the hydrogen spectrum had linewidths of ~ 0.4 Hz. Consequently, the hydrogen signals decayed very slowly and we were able to pick a 150 ms portion of the absolute magnitude that remained flat within 1%.

The carbon spin dynamics consisted of a series of delays interleaved with pulses. During the delays the spins evolved under the internal Hamiltonian. The pulse flip angles were randomly sampled from a uniform distribution that ranged between $-\pi/20$ and $\pi/20$ about the y axis. A cycle time of 1 ms was defined, within which the kick frequency ranged from 3 kicks/cycle to 30 kicks/cycle in steps of 3 for a total of ten different kick frequencies. The range of the kick frequency was limited by the shortest pulse the spectrometer was capable of generating, which is 100 ns. The time alloted for a sequence of one delay period followed by a pulse was given by the cycle time/(number of kicks/cycle). Within this sequence the delay time is given by the total sequence time minus the pulse-on time. The maximum pulse-on time was 10 μs which corresponded to the maximum flip angle of $\pi/20$. The nutation frequency for this rf field was 2500 Hz. (Compare this to the chemical shifts of the carbons which were separated by 1260 Hz.) For a given kick frequency, the length of the series of successive sequences of delay plus pulse, generated as described above, fit the total acquistion time of 150 ms.

The experiments were run for ten different kick frequencies with an average over 50 realizations. A waiting time of 300 s was used between successive realizations. Figure 8 shows the result of the experiments. The absolute magnitudes of these plots were fitted to an exponential. The χ^2 per degree of freedom for the 10 fits ranged from 1.1 to 8.5. The χ^2 fit the average decays well but do not account for the details in the fine structure evident from the oscillations of the magnitudes. As the kick frequency increases the data demonstrates that the system is decohered faster. A plot of the decay constants as a function of kick frequency, Fig. 9, shows this trend clearly. The experimental results seem to exhibit revivals in the higher kick rates of Fig. 9. But this is due to low statistics (see Fig. 5).

V. DISCUSSION

We have described a method for modeling decoherence that requires only limited quantum resources and implemented the model on a NMR QIP. The key feature of the model which enables simulation of the dephasing effects and the attenutation of recurrences normally produced by a much larger quantum environment is the application of classical kicks to randomize the information in the environment states. Although the quantum system and environment dimensions are small and remain fixed, the system state exhibits an irreversible loss of coherence due to an averaging over the random realizations of kicks to the environment states. In particular, in the case of a $\sigma_z\sigma_z$ system-environment interaction, we have shown that the kick frequency can be varied to control the decay rate of the phase damping. Although in this paper we have focused on the simulation of continuous phase damping, the model can be immediately generalized to other system-environment couplings and the resultant decoherence channels. A major advantage of this model is that it provides a procedure through which the mechanisms of decoherence can be explored using techniques currently available in NMR QIP.

As resources permit, the model we have described may be generalized to simulate and study a wider variety of decoherence channels and system-environment couplings. In particular, the ''nearest'' quantum environment need not be the only quantum environment. For example, in order to implement a time-varying decoherence process with a fixed set of system-environment couplings it may be advantageous to introduce an environment ''hierarchy'' (see Fig. 1 for a schematic). The idea here is to couple the first quantum environment to a second, larger environment (through another set of fixed bilinear couplings), and so on. The dimension of the next Hilbert space in the environment hierarchy may be limited to N^2, where N is the dimension of the Hilbert space of the immediately smaller system. In this framework only the nearest environment remains directly coupled to the system of interest. The approximation of using stochastic classical fields to reduce unwanted back action may then be applied to the final quantum environment, which is much more remote from the system of interest.

In conclusion, we have developed a model that is practical for simulating quantum decoherence effects associated with a time-independent superoperator on a QIP device. By varying the phase kicking rate in the stochastic Hamiltonian we can control the system's phase-damping rate. In this presentation we have shown the effectiveness of the methodolgy, in the case of one- and two-spin environments, using analytical solutions, numerical simulations, and a physical implementation on a NMR QIP device. These methods have illustrated the use of stochastic kick rates on the quantum environment for controlling system decoherence rates and recurrence times.

ACKNOWLEDGMENTS

We thank L. Viola and E. Farhi for helpful discussions. This work was supported by the U.S. Army Research Office under Grants No. DAAD 19-01-1-0519 and No. DAAD 19-01-1-0678 from the Defense Advanced Research Projects Agency. J.P.P. acknowledges support from Anpcyt, Ubacyt, and Fundacion Antorchas.

[1] J. von Neumann, *Mathematische Grundlagen der Quantenmechanik* (Springer, Berlin, 1932), Chaps. V and VI; English translation by R. T. Beyer, *Mathematical Foundations of Quantum Mechanics* (Princeton University Press, Princeton, 1955).
[2] W. H. Zurek, Phys. Today **44**, 36 (1991).
[3] D. Giulini, E. Joos, C. Kiefer, J. Kupsch, I.-O. Stamatescu, and H. D. Zeh, *Decoherence and the Appearance of a Classical World in Quantum Theory* (Springer, Berlin, 1996).
[4] J. P. Paz and W. H. Zurek, in *Coherent Matter Waves*, Proceeding of the Les Houches of Theoretical Physics, Session LXXII, edited by R. Kaiser, C. Westbrook, and F. David (Springer, Berlin, 2001), pp. 533–614.
[5] W. H. Zurek, Phys. Rev. D **26**, 1862 (1982).
[6] W. H. Zurek, S. Habib, and J. P. Paz, Phys. Rev. Lett. **70**, 1187 (1993).
[7] J. P. Paz and W. H. Zurek, Phys. Rev. Lett. **82**, 5181 (1999).
[8] J. E. Poyatos, I. Cirac, and P. Zoller, Phys. Rev. Lett. **77**, 4728 (1997); A. R. R. Carvalho, P. Milman, R. L. de Mattos Filho, and L. Davidovich, *ibid.* **86**, 4988 (2001); J. P. Paz, Nature (London) **412**, 869 (2001).
[9] J. P. Paz, S. Habib, and W. H. Zurek, Phys. Rev. D **47**, 488 (1993); J. R. Anglin, J. P. Paz, and W. H. Zurek, Phys. Rev. A **55**, 4041 (1997).
[10] G. M. Palma, K.-A. Suominen, and A. K. Ekert, Proc. R. Soc. London, Ser. A **452**, 567 (1996).
[11] L. Viola and S. Lloyd, Phys. Rev. A **58**, 2733 (1998).
[12] A. J. Legget, S. Chakravarty, A. T. Dorsey, M. P. A. Fisher, A. Garg, and W. Zwerger, Rev. Mod. Phys. **59**, 1 (1987).
[13] E. Knill and R. Laflamme, Phys. Rev. A **55**, 900 (1997).
[14] E. Knill, R. Laflamme, and L. Viola, Phys. Rev. Lett. **84**, 2525 (2000).
[15] L. Viola, E. M. Fortunato, M. A. Pravia, E. Knill, R. Laflamme, and D. G. Cory, Science **293**, 2059 (2001).
[16] E. M. Fortunato, L. Viola, J. Hodges, G. Teklemariam, and D. G. Cory, New J. Phys. **4**, 1 (2002).
[17] C. Cohen-Tannoudji, J. Dupont-Roc, and G. Grynberg, *Atom-Photon Interactions: Basic Processes and Applications* (Wiley, New York, 1992).
[18] J. Preskill (unpublished).
[19] B. Schumacher, Phys. Rev. A **54**, 2614 (1996).
[20] K. Kraus, *States, Effects and Operations: Fundamental Notions of Quantum Theory* (Springer, Berlin, 1983).
[21] M. A. Nielsen and I. L. Chuang, *Quantum Computation and Quantum Information* (Cambridge University Press, Cambridge, U.K., 2000), Chap. 8.
[22] T. F. Havel, Y. Sharf, L. Viola, and D. G. Cory, Phys. Lett. A **280**, 282 (2001).

[23] S. S. Somaroo, C. H. Tseng, T. F. Havel, R. Laflamme, and D. G. Cory, Phys. Rev. Lett. **82**, 5381 (1999).
[24] C. H. Tseng, S. S. Somaroo, Y. Sharf, E. Knill, R. LaFlamme, T. F. Havel, and D. G. Cory, Phys. Rev. A **61**, 012302 (2000).
[25] J. S. Waugh, J. Magn. Reson. **50**, 30 (1982).
[26] H. Green and R. Freeman, J. Magn. Reson. **93**, 141 (1991).
[27] R. Freeman, *Spin Choreography* (Oxford University Press, Oxford, U.K., 1998).